Decomposition of SiH_3 to SiH_2 on Si(100)-(2×1)

Freda C. H. Lim,[1] E. S. Tok,[2] and H. Chuan Kang[1,*]
[1]*Department of Chemistry, National University of Singapore, 10 Kent Ridge Crescent, Singapore 119260, Singapore*
[2]*Department of Physics, National University of Singapore, 10 Kent Ridge Crescent, Singapore 119260, Singapore*
(Received 10 May 2006; revised manuscript received 21 August 2006; published 28 November 2006)

The decomposition energetics of the silyl group into silylene and hydrogen on the Si(100)-(2×1) surface was studied using pseudopotential density functional calculations. The results provided insight on the relative stability of the adsorption configurations of silylene in the presence of different coverages of coadsorbed hydrogen. We find that the prevalence of the intrarow silylene on the growth surface is a result of both thermodynamics and kinetics. Our results also suggest that both the silylene group and the hydrogen atom formed by silyl decomposition acquire frustrated translational energy in the exit valley of the decomposition pathway. In particular, the hydrogen atom is approximately 0.5 eV more energetic than the thermal energy. This is consistent with observations made in scanning tunnel microscope images that show the dissociating hydrogen atom migrating away from the decomposition site.

DOI: 10.1103/PhysRevB.74.205333 PACS number(s): 68.43.Bc, 68.47.Fg, 68.43.Fg

I. INTRODUCTION

As dimensions of semiconductor devices scale down with the prediction of Moore's law, the effects of reconstructions and defects on their performance will become increasingly important. It is therefore important to have a clear understanding of the molecular scale processes occurring during the growth of these materials in order to achieve better control of the material properties. Silicon is an important material in the semiconductor industry because of the well-established complementary metal-oxide semiconductor (CMOS) technology. Although trends are slowly moving towards developing alternate materials for devices, a better understanding of the silicon growth process will also help to shed light upon the growth process of other related material such as silicon-germanium and strained silicon. Silane and disilane are common gas source precursors used in the gas source molecular beam epitaxy (GSMBE) of silicon.[1] As such, investigations of the decomposition of these gas source precursors leading to growth of Si have thus been studied

The first step in this decomposition involves the formation of the silyl group. Its subsequent decomposition to the silylene group has been investigated by a number of groups. The equilibrium adsorption sites of the silylene are now rather well established.[2–7] Without adsorbed hydrogen atoms in the vicinity of the silylene group, the most favorable adsorption configuration is the on-dimer structure with the silylene adsorbed onto a surface dimer leaving the surface dimer σ bond intact. With hydrogen atoms coadsorbed in the vicinity of the silylene, the more stable configuration is the intrarow structure with the silylene adsorbed on one side of the dimer row between two neighboring dimers. Two other structures that have also been considered are the in-dimer structure and the inter-row structure. The former is similar to the on-dimer structure except that the σ bond of the dimer is broken. The latter consists of a silylene group adsorbed between two dimers on neighboring dimer rows. These adsorption configurations are illustrated in Fig. 1.

The energetics of these silylene configurations has been well studied by theoretical methods. Earlier density functional theory (DFT) calculations have shown that the inter-row configuration and in-dimer configuration have energies that are higher than the intrarow configuration and the on-dimer configuration.[2] Thus, much of the later theoretical work was focused on resolving the energy difference the latter two configurations. On the clean surface, all the calculations reported in the literature indicate that the on-dimer configuration is at least as stable as, if not more stable than, the intrarow configuration.[2–5] However, the on-dimer configuration is not experimentally observed even at room temperature and (silane or disilane or SiH2 or H) total coverages of silylene and hydrogen below 0.1.[6,7] Bowler and Goringe[2] argued against the on-dimer configuration based on the strong repulsive lateral interaction calculated for two such groups on nearest-neighbor dimers along a dimer row. Their calculations, on the other hand, showed no strong repulsive interactions for two intrarow groups. However, the effects of lateral interactions are expected to be small for sufficiently

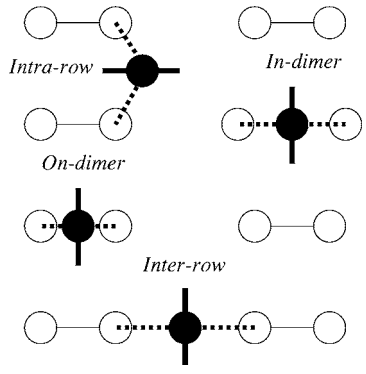

FIG. 1. An illustration of possible adsorption sites of the silylene group. Black circles indicate the silicon atom of the silylene group. Thick lines represent the two hydrogen atoms of the silylene group. Empty circles indicate the silicon atoms of the dimer. Dashed lines indicate the bonds between silylene and surface silicon atoms. The difference between the on-dimer and the in-dimer configuration is that in the former, only the π bond of the dimer is broken while in the latter, both the σ bond and the π bond of the dimer are broken to accommodate the silylene insertion.

low coverages. An additional factor that is important is the presence of coadsorbed hydrogen. Since decomposition of the silyl group leads to adsorbed hydrogen, it makes sense to study the relative stabilities of these in the silylene configurations with one or more coadsorbed hydrogen atoms in the vicinity. More recent calculations revealed that in the presence of coadsorbed hydrogen, the relative stabilities of the two configurations are reversed.[3–5]

Although the adsorption sites are well established, the decomposition pathway from silyl to silylene is still not resolved. Surface analysis techniques such as secondary-ion-mass spectroscopy (SIMS), temperature-programmed desorption (TPD), and low-energy electron diffraction (LEED) have been used by Gates *et al.* to study the decomposition mechanism of SiH_x species on the Si(100)-(1×2) surface.[8–11] This work, as well as many others,[6,7,12–18] shows that the silyl group produced by the decomposition of silane and disilane is metastable and has an average lifetime on the order of a few minutes at room temperature.[6] Scanning tunnel microscopy (STM) studies also show that the silylene group resulting from silyl decomposition remains stable below 470 K.[19] Silylene is therefore believed to be the predominant species occurring on Si(100)-(1×2) during growth by GSMBE. The adsorbed silyl group interacts with two dangling bonds on the surface to give rise to a silylene group and a hydrogen atom, the decomposition rate depending upon the dangling bond coverage in the vicinity. From temperature-programmed SIMS data and using the analysis in Refs. 20 and 21, the activation barrier for silyl decomposition was estimated to range from 0.08 eV at saturation silane dosage to 0.1 eV at low silane dosage. The corresponding pre-exponential factors are rather low at 0.7 s^{-1} and 4 s^{-1}, respectively. These results led Gates *et al.* to conclude that the decomposition rate is limited by the availability of dangling bonds on the surface.

Two theoretical studies have calculated the activation barrier of silyl decomposition process. Density functional theory calculations using cluster models[22] find a low barrier of 0.25 eV when the process is assisted by atomic hydrogen leading to an in-dimer structure (but a rather higher barrier of 1.43 eV without hydrogen-abstraction assistance). However, the hydrogen-abstraction assisted process proposed in Ref. 16 does not involve the participation of dangling bonds, and is thus not consistent with the experimental data that established a dependence upon the dangling bond coverage. The activation barrier of 0.25 eV is relative to a reactant state that includes a hydrogen atom in the gas phase. In the transition state, the dimer bond is broken (ring opening) but the activation barrier is not large because the transition state includes a gas phase hydrogen molecule formed from the reactant hydrogen atom. In addition, there are a couple of points that should be noted here. It has been shown in earlier calculations[2] using slab models of the surface that the in-dimer structure resulting from the proposed hydrogen-abstraction assisted process is less stable than the intrarow structure by about 0.2 eV.[2] Furthermore, the cluster models used in Ref. 16 only have one dimer along each dimer row and thus are not able to probe the intrarow model at all. Even though the activation barrier found is low and is somewhat in agreement with the experimental data in Refs. 8–11, the pathway identified seems problematic.

A more recent DFT slab calculation modeled within a generalized gradient approximation (GGA) by Smardon and Srivastava[23] discusses the decomposition of silane and disilane and the subsequent decomposition of the resulting silyl species. They reported a barrier of 2 and 2.5 eV for the low-hydrogen ambience decomposition pathway of silyl decomposition to the intrarow and on-dimer respectively. While there is an apparent preference for the intrarow pathway under low-hydrogen ambience, the preference is reversed in the case where fragmented hydrogen is present with a 1.0 eV difference in the decomposition barrier. This is despite the intrarow configuration being found to be 0.1 eV more energetically stable than the on-dimer configuration.

There is also experimental evidence for silyl decomposition leading to the intrarow structure from STM at low disilane coverage.[6,7] In the sequential images of Si(100)-(1×2), the adsorption of the silyl group and its subsequent dissociation reaction into intrarow silylene and hydrogen have been observed. However, this is not conclusive evidence for a pathway leading directly from adsorbed silyl to the intrarow configuration as the latter can also be formed from the relaxation of the silylene group from a higher energy configuration after the decomposition process. Subsequently, data from various other groups also supported the decomposition of the silyl group into the intrarow site through different experimental means. The absence of a symmetry axis perpendicular to the surface as indicated by multiple internal reflection infrared spectroscopy (MIR-IRS) polarized radiation measurements[18] points to the fact that vibration is tilted, consistent with the intrarow configuration. With a combination of MIR-IRS and density functional theory cluster calculations, it has also been shown that the calculated stretching frequencies of the intrarow configuration are in good agreement with the experimentally observed modes.

In this paper, we present density functional slab calculations of the silyl group decomposition pathways leading to on-dimer and intrarow silylene structures. Comparison of calculated energetics of the silylene configurations on a clean Si surface or with one or more coadsorbed hydrogen atoms in the vicinity will be useful in providing further insight into the molecular pathways for the silyl decomposition. Thus far, the generalized gradient approximation has been used in one previous study.[23] Our calculations could also serve as useful comparisons with previous calculations using the local density approximation (LDA).[2–5] We find that the resulting intrarow silylene on the growth surface is a result of both thermodynamics and kinetics.

II. CALCULATION METHOD

We use density functional pseudopotential plane wave calculations. The Si(100)-(2×1) surface is modeled using a slab that contains six layers of Si atoms. The topmost five layers are fully relaxed without any constraints, while atoms in the bottom layer are fixed at ideal bulk positions. Dangling bonds at the bottom of the slab are terminated with hydrogen. The vacuum thickness is approximately 10 Å. We used the following supercell sizes in our calculations: (2×2),

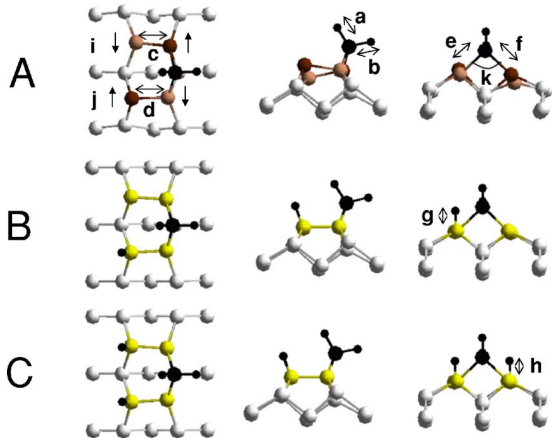

FIG. 2. (Color online) Illustration of the silylene group adsorbed in the intrarow configuration without any neighboring hydrogen atom (structure *A*), with one co-adsorbed hydrogen atom (structure *B*) and with two co-adsorbed hydrogen atoms (structure *C*). The labels *a* to *k* indicate the lengths and angles given in Table I. Buckled up atom on dimmer (dark brown); buckled down atom in dimmer (light brown); un-buckled dimmer (yellow).

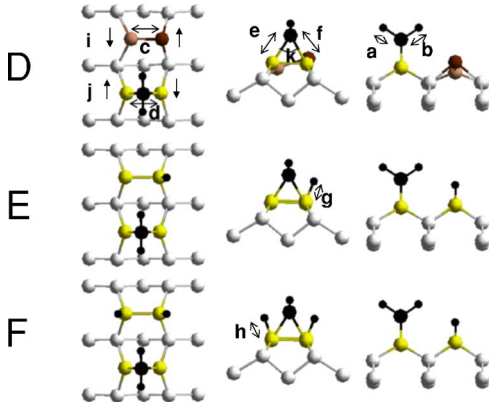

FIG. 3. (Color online) Illustration of the silylene group adsorbed in the on-dimer configuration without any neighboring hydrogen atom (structure *D*), with one coadsorbed hydrogen atom (structure *E*) and with two co-adsorbed hydrogen atoms (structure *F*). The bond lengths and angles denoted by *a* to *k* are given in Table I.

(2×4), and (4×2). The ionic and electronic degrees of freedom are relaxed using a conjugate-gradient algorithm.[24] Electron exchange correlation is approximated with the Perdew-Burke-Ernzerhof generalized gradient approximation functional.[25] The silicon ion cores are treated using completely separable norm-conserving nonlocal pseudopotentials in the Kleinman-Bylander form.[26] The hydrogen atoms were treated using the full $1/r$ potential. The cutoff radius for each of the *s*, *p*, and *d* channels is 0.95 Å. The Kohn-Sham equations are solved using a plane wave basis set with a cutoff energy of 20 Ry and electronic states were sampled at 4 *k* points, namely $(0,\pm1/4,\pm1/4)$ for the 2×2 and 2 *k* points, namely $(0,0,\pm1/4)$ for the 2×4 supercell and $(0,\pm1/4,0)$ for the 4×2 supercell. The first direction is along the dimer bond, the second is along the dimer row, and the third is perpendicular to the slab surface.

III. RESULTS AND DISCUSSION

A. Structure

We first discuss the structure and energetics of the intrarow and on-dimer adsorption states for silylene. Then we present results for the decomposition paths to get from the silyl group to each of these silylene adsorption states. Figures 2 and 3 illustrate the structures of interest for the intrarow configuration and the on-dimer configuration, respectively, with different numbers of coadsorbed hydrogen atoms. Some bond lengths and bond angles are summarized in Table I. Adsorption onto the dimer weakens the dimer bond. This can be seen in the increase in the dimer bond lengths after adsorption. From our calculations, the clean dimer bond length is 2.35 Å, while the dimer bond length for the on-dimer structure is 2.42, 2.45, and 2.43 Å with zero, one, and two hydrogen atoms adsorbed on the neighboring dimer. For the intrarow configuration, the dimer bond lengths for the adsorbing dimer pair are 2.38 and 2.44 Å when no hydrogen atoms are coadsorbed on the dimer-pair (structure *A*). Both dimers are buckled. When the dimer pair is coadsorbed with hydrogen atoms, the bond lengths are both 2.41 Å and there is no buckling. Thus, as expected, in both the on-dimer and the intrarow configurations, adsorption weakens the dimer bond significantly. This is readily rationalized in terms of the weakening of the π bond when adsorption occurs. Adsorption at the on-dimer site leaves no extra dangling bonds behind, while adsorption at the intrarow site leaves two dangling bonds at the other end of the dimer pair, leading respectively to the formation of a three-member and a four-member ring structure. When there is no neighboring hydrogen coadsorption, the adsorbed dimers are buckled for adsorption at both intrarow and on-dimer sites. However, the buckling angles are smaller than those for the clean surface. The angle (~60° for on-dimer and ~90° for intrarow) between the two silylene-surface bonds is rather different from the tetrahedral angle, thus suggesting that these ring structures are probably highly strained structures.

TABLE I. Bond lengths and bond angles for the intrarow and the on-dimer configurations illustrated in Figs. 1 and 2. Lengths *a*–*h* are angstroms, angles *i* and *j* are in degrees.

	A	B	C	D	E	F
a	1.523	1.523	1.524	1.514	1.515	1.516
b	1.522	1.521	1.522	1.514	1.515	1.516
c	2.376	2.388	2.410	2.321	2.403	2.412
d	2.442	2.406	2.410	2.421	2.445	2.434
e	2.411	2.423	2.427	2.329	2.331	2.334
f	2.433	2.423	2.426	2.336	2.329	2.333
g	···	1.523	1.524	···	1.522	1.523
h	···	···	1.524	···	···	1.523
i	14.3	4.9	3.8	18.5	0.5	0.0
j	7.3	3.5	3.7	1.0	0.4	0.1
k	91.6	91.1	91.0	62.7	63.3	62.9

TABLE II. A summary of the methods previously used and the relative adsorption energetics of the on-dimer and intrarow configuration on clean and coadsorbed silicon surfaces.

	Bowler and Goringe (Ref. 2)	Hong and Chou (Ref. 3)	Camak and Srivastava (Ref. 4)	Takeuchi (Ref. 5)	Smardon and Srivastava (Ref. 23)	Our work	Our work	Our work
Slab Thickness	5 layers Si	6 layers Si	8 layers Si	5 layers Si	8 layers Si	6 layers Si	6 layers Si	6 layers Si
method	DFT/LDA	DFT/LDA	DFT/LDA	DFT/LDA	DFT/GGA	DFT/GGA	DFT/GGA	DFT/GGA
E_{cut}/Ryd	14.7	10	8	10	10	20	20	20
Supercell size	2×2	$p(\sqrt{8}\times\sqrt{8})R45°$	2×2	4×4	2×2	2×2	2×2	2×4
No. k points	Not reported	2	3	1	4	1	4	2
ΔE (SiH_2)[a]	0.004	−0.14	−0.10	−0.26	⋯	−0.04	−0.04	−0.18
ΔE (SiH_2+H)[a]	⋯	0.13	0.15	⋯	⋯	0.05	0.13	0.15
ΔE (SiH_2+2H)[a]	⋯	0.11	−0.08	0.11	0.1	0.09	0.15	⋯

[a]ΔE=E(on-dimer)−E(intra-row).

Indeed, the on-dimer structure was ruled out by early work on the basis of the small bond angle.[7] It is interesting to note that the adsorption of an on-dimer silylene group on a dimer leaves the adjacent clean dimer slightly shortened.

B. Energetics

Table II is a summary of adsorption energetics, including results obtained in previous calculations. We will briefly discuss the relative stabilities of the silyl decomposition products before we look at the activation energies for silyl decomposition. Our results are in good agreement with what has been previously reported in the literature.[2–5,23] In the present study, two different supercell sizes are used. The 2×2 supercell consists of two dimers in a single dimer row. Thus, a calculation of the intrarow structure using this supercell unavoidably includes the interaction between an intrarow silylene and the next intrarow silylene adsorbed on the next dimer pair along the same dimer. The 2×4 supercell consists of four dimers along a single dimer row. Here, the lateral interaction is less than that present in the 2×2 supercell since the silylene groups are separated by two dimers from its nearest neighbor along the dimer row. The same considerations apply for the on-dimer configuration. Without hydrogen coadsorption, our calculations with the 2×2 supercell show a small energy difference $\Delta E=E_A-E_D$ of 0.04 eV between the less stable intrarow (structure A) and the more stable on-dimer (structure D) configurations. The relative stability is in agreement with most previous calculations[3–5] although these calculations show a significantly larger energy difference. Çakmak and Srivastava,[4] using a 2×2 supercell found $\Delta E=0.10$ eV with a local density approximation, while the earlier calculations[2] also using a 2×2 supercell found an energy difference of 0.004 eV. Our 2×2 supercell results are probably more in line with the conclusion that the energy difference between these two structures is small.[2] However, with the 4×2 supercell where the energetics are less likely to be affected by lateral interactions, a larger energy difference of 0.18 eV is observed. This compares reasonably well with Hong and Chou[3] as well as Takeuchi,[5] who found $\Delta E=0.14$ eV and 0.26 eV, respectively, using the local density approximation. Our results show that a sufficiently large supercell size is required to obtain an accurate comparison for these structures. Considering the change in the buckling of the dimers as a result of adsorption, lattice effects probably contribute quite significantly to this lateral interaction. A comparison of the results of previous LDA calculations from two different groups,[4,5] one with a 2×2, and the other with a 4×4 supercell suggests the same conclusion. The on-dimer configuration was found to be more stable by 0.10 eV and 0.26 eV, respectively. The relative stability of the on-dimer configuration can be understood from the analysis of the configurations. As mentioned in Sec. III A, the adsorption at the on-dimer site leaves no extra dangling bonds behind, while adsorption at the intrarow site leaves two dangling bonds at the other end of the dimer pair. These additional dangling bonds are believed to give rise to the energy difference. We note that the LDA energy difference is larger than our GGA result.

On the clean surface, the on-dimer configuration is energetically more favorable than the intrarow configuration. However, in the presence of coadsorbed hydrogen, our calculations show that the intrarow configuration (structure C) now is more stable than the on-dimer configuration (structure F). This reversal in relative stabilities of the on-dimer and the intrarow configurations can be attributed to the saturation of the additional dangling bonds formed by the intrarow configuration when hydrogen is coadsorbed. With the saturation of the dangling bonds, the strained induced in the three or four-membered ring structures becomes the deciding factor for relative stabilities. This result is consistent with all but one previously reported calculations. The hydrogen coadsorption calculation performed by Çakmak and Srivastava[4] predicted the opposite relative stability. Their calculation uses a small (2×2) supercell along with the local density approximation and, from our discussion above, the (2×2) supercell calculation is probably affected by lateral interactions. Thus a sufficiently large supercell size is required to obtain an accurate comparison for these structures.

The greater stability of the intrarow structure implies that decomposition leads to the intrarow configuration since at

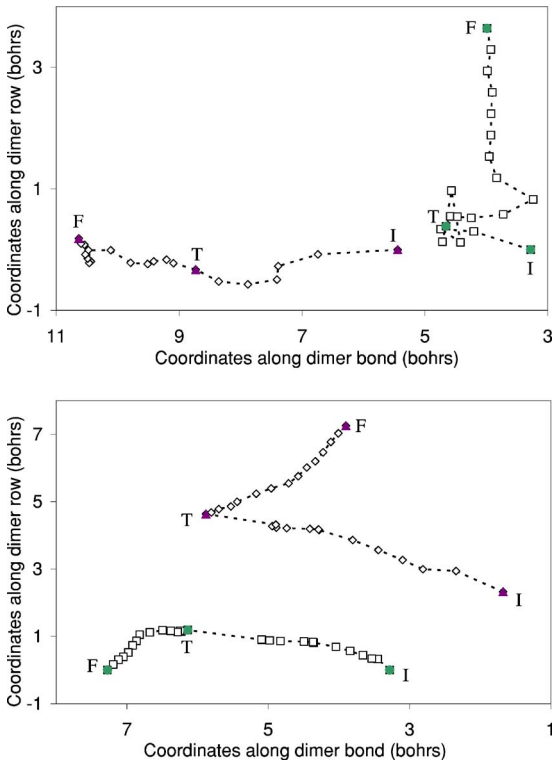

FIG. 4. (Color online) The positions of the silyl group (□) and the hydrogen atom (◇) along the decomposition path to (a) the intrarow configuration, and (b) the on-dimer configuration. The initial, transition, and final states are denoted by *I*, *T*, and *F*, respectively.

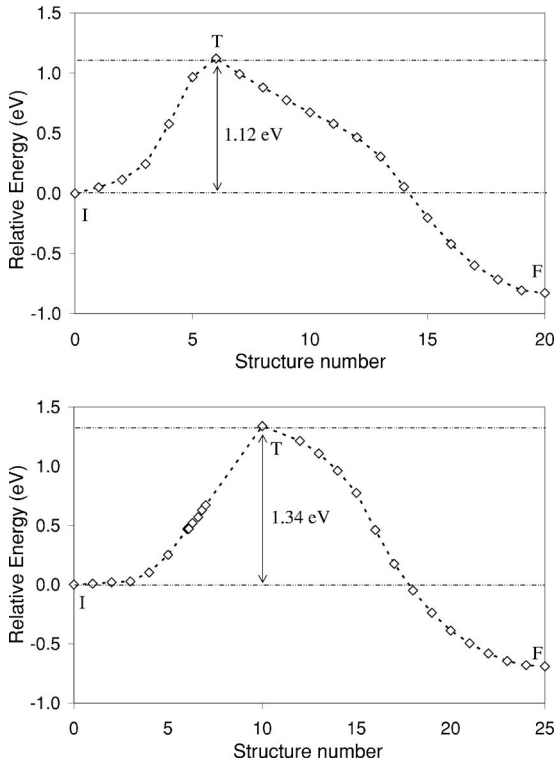

FIG. 5. Plots of energy versus structure number for (a) the intrarow path and (b) the on-dimer path. For both paths, structure 0 corresponds to the initial structure. The initial, transition, and final states are denoted by *I*, *T*, and *F*, respectively.

least one hydrogen atom would be coadsorbed in the vicinity of the silylene group immediately after it is formed. As suggested in the STM study by Bronikowski *et al.*,[7] hydrogen can subsequently diffuse away, leaving silylene adsorbed in the intrarow configuration. We discuss this further in the next section.

C. Decomposition paths

In this section we discuss our calculations of the activation barrier for silyl decomposition into the silylene and hydrogen. The results obtained here provide evidence that the formation of the on-dimer configuration, other than being thermodynamically unfavorable, is also kinetically hindered. In order to trace the decomposition paths, optimized geometries were obtained for a number of structures in each of which the distance $d_{\text{Si-H}}$ between the silyl silicon atom and its dissociating hydrogen atom is held fixed at different values. A total of 21 (26) different structures were computed for the path leading to the intrarow (on-dimer) configuration. The positions of the silyl silicon atom and the dissociating hydrogen atom in the plane of the surface are plotted in Fig. 4 for both intrarow (a) and on-dimer paths (b), with the transition state for each indicated. The results for energetics are summarized in Fig. 5, where the energy for each structure along the path is plotted. The same data is plotted in Fig. 6 to show the dependence upon $d_{\text{Si-H}}$. The activation barrier for the silyl group to decompose to the intrarow silylene is found to be 1.12 eV and that to decompose to the on-dimer silylene is found to be 1.34 eV.

The decomposition barrier of the silyl group has also been studied[22] with cluster models of the silicon surface, which use more reliable methods of locating the transition point than the reaction path tracing that we use here. In Ref. 22 the decomposition barrier of a silyl group into a silylene group and a hydrogen atom adsorbed on the same dimer are calculated to be approximately 1.12 eV using a three-dimer trench cluster. This cluster model of the surface consists of three adjacent dimers in the direction perpendicular to the dimer row. The reaction path includes an intermediate state with a hydrogen atom and a silylene group adsorbed on a dimer.

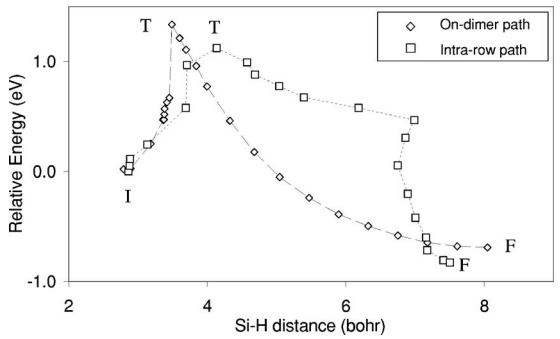

FIG. 6. Plots of energy vs Si-H distance for the intrarow path (□) and the on-dimer path (◇). The initial, transition, and final states are denoted by *I*, *T*, and *F*, respectively.

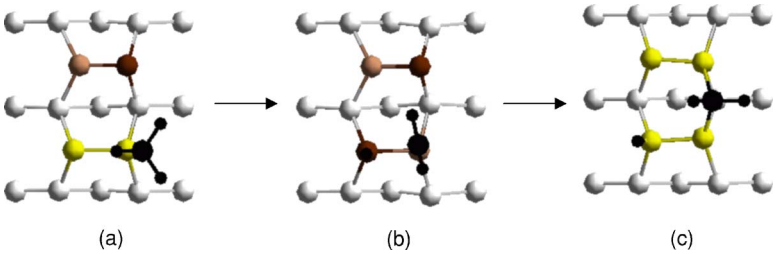

FIG. 7. (Color online) Structures of the (a) reactant, (b) transition, and (c) product states for the intrarow path.

The latter forms an on-dimer structure through a dimer-breaking and ring-formation process that has a barrier of 1.12 eV. Our slab calculations, however, show that the intermediate structure in these cluster calculations is actually unstable (as opposed to being metastable) if there is an adjacent dimer in the direction of the dimer row; the silylene group bonds to the silicon atom in the adjacent dimer (along the dimer row) to form the intrarow structure. In the cluster model used, this instability is not observed probably because the model consists of only one dimer in the dimer of the dimer row. Thus, cluster model size is particularly important here. Indeed, both the reaction paths we investigate in this paper probably require a least a four-dimer trench cluster model with two dimers to model each of two adjacent dimer rows. To the best of our knowledge, there are currently no cluster calculations with models that are sufficiently large to probe the reaction paths we study here.

It is quite clear from the results in Figs. 4 and 5 that the reaction coordinate is not simply the silicon-hydrogen distance $d_{\text{Si-H}}$. In particular, a graphical illustration of this is seen in Fig. 7 where the structures of the silyl group (a), the transition state (b), and silylene (c) are compared for the intrarow path. In the transition state, the hydrogen atom is already quite close to its final position in the decomposition process. However, the position of the silylene group is still quite far from its final position in the process. That is, the entry "valley" of the decomposition path is mainly defined by the dissociation of the hydrogen atom from the silyl silicon, whereas the exit "valley" is mainly defined by the formation of the bond between the silylene group and the silicon atom on the neighboring dimer. We will discuss this further below in relation to an estimate of the vibrational energies imparted to the hydrogen atom and the silylene group as a result of the decomposition. Since the difference in the activation barriers is 0.22 eV, assuming the same pre-exponential factors, the ratio of the rate of formation of the intrarow structure C to the rate of formation of the on-dimer structure F is approximately 5000. At 573 K, the rate of forming structure C would still be approximately 85 times faster than the rate of forming structure F. Thus our results show that the intrarow configuration is favored both energetically and kinetically. The difference in the activation barriers is actually larger than the difference in the energies of the two configurations.

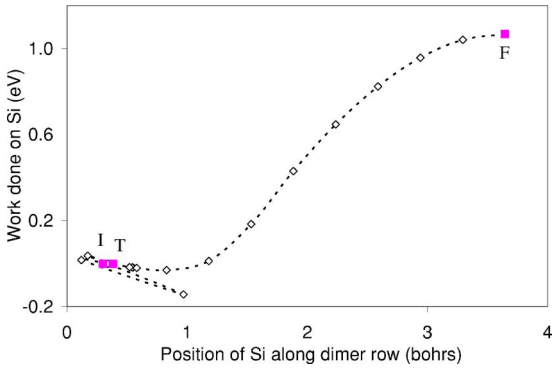

FIG. 8. (Color online) A plot of work done on the silicon atom in the [110] direction along the dimer row during the silyl decomposition into the intrarow silylene group. The initial position, transition state, and its final position are as indicated on the plot as I, T, and F, respectively. It can be seen from the plot that the silylene species gains energy as it moves in the direction of the dimer row after it breaks apart from the silyl species.

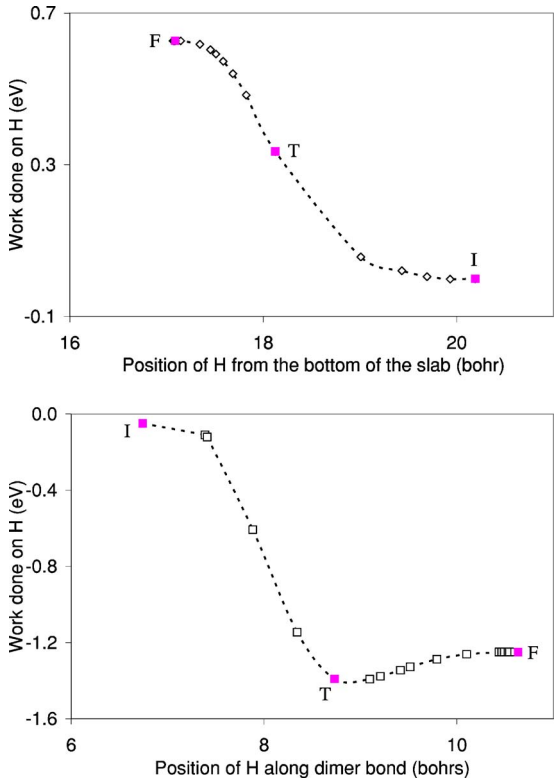

FIG. 9. (Color online) Plots of work done on the hydrogen atom that dissociated from the silyl group during the decomposition process: (a) work done in moving the hydrogen atom closer to the surface; (b) work done in moving the hydrogen atom in the direction along the dimer bond. Its initial position, transition state, and its final position are as indicated on the plot as I, T, and F, respectively. It can be seen from both plots that the atomic hydrogen gains energy in the exit channel of the dissociation path.

As we have seen above, the silicon-hydrogen distance $d_{Si\text{-}H}$ is large at the transition state with the hydrogen atom already close to its final position in the product well. Thus, a significant amount of the energy needed to reach the transition state must go into this silicon-hydrogen bond stretching. We attempt to address the question of how this energy is partitioned into the various degrees of freedom of the decomposition products after the system passes the transition state. This is done by calculating, within a classical mechanical approximation, the frustrated translational energies acquired by the hydrogen atom and the silylene fragment in the exit valley of the reaction path. The work done on the fragments by the potential energy surface is plotted in Figs. 8 and 9 for the silylene and the hydrogen atom, respectively. As the system passes from the transition state to the decomposition product state, both the hydrogen atom and the silylene group acquire a significant amount of energy. In the exit valley, the force acting on each of the hydrogen atom and the silylene group is in the same direction as the displacement. We assume that beyond the transition state the silylene and hydrogen atoms are sufficiently decoupled from each other that they do not exchange energy. This estimate of the energy acquired in the exit channel is a rather rough estimate since we are essentially following the bottom of the minimum energy path, and hence do not take into consideration the dynamical coupling of the hydrogen and silylene motion to the phonon bath. The silylene-surface and hydrogen-surface bonds are roughly of the same strength, but the hydrogen mass is much smaller so that this approximation may be better for hydrogen than for the silylene group. Within this approximation, the results in Figs. 8 and 9 suggest that the decomposition process produces a hydrogen atom that is approximately 0.5 eV more energetic than the average thermal energy. This is consistent with STM observations,[7] showing noncorrelated positions of the silylene species and the hydrogen atoms, suggesting mobility of these species right after silyl decomposition.

The on-dimer configuration has not been observed experimentally to the best of our knowledge. This is despite its energy being lower than the intrarow configuration in the absence of neighboring coadsorbed hydrogen. Our results support the following scenario for silyl decomposition. First, the silyl group decomposes into intrarow silylene rather than an on-dimer silylene because of the more favorable kinetics. Then the hydrogen atom diffuses away, leaving an isolated silylene that is trapped in the intrarow configuration.

IV. CONCLUSION

In conclusion, we have investigated two possible dissociation pathways from adsorbed silyl to silylene and hydrogen. Our results show that the intrarow adsorption site is favored over the on-dimer adsorption site for the silylene group, for both thermodynamic and kinetic reasons. The activation barrier for forming silylene at the on-dimer site is 0.22 eV higher than at the intrarow site. Our calculations show that the adsorption energy at the intrarow site is larger by 0.18 eV, in agreement with previous calculations that also favor the intrarow site thermodynamically. Analysis of the forces acting on the dissociating silyl group in the exit channel of the intrarow path shows that the hydrogen atom and the silylene groups are both significantly energetic after the dissociation process thus providing support for the transient mobility of the hydrogen atom.

*Corresponding author. Email address: chmkhc@nus.edu.sg

[1] K. Werner, S. Butzke, S. Radelaar, and P. Balk, J. Cryst. Growth **136**, 322 (1994).
[2] G. R. Bowler and C. M. Goringe, Surf. Sci. **360**, L489 (1996).
[3] S. Hong and M. Y. Chou, Phys. Rev. B **58**, R13363 (1998).
[4] M. Çakmak and G. P. Srivastava, Phys. Rev. B **61**, 10216 (2000).
[5] N. Takeuchi, Surf. Sci. **529**, 274 (2003).
[6] Y. Wang, M. J. Bronikowski, and R. J. Hamers, Surf. Sci. **311**, 64 (1994).
[7] M. J. Bronikowski, Y. Wang, M. T. McEllistrem, D. Chen, and R. J. Hamers, Surf. Sci. **298**, 50 (1993).
[8] S. M. Gates, C. M. Greenlief, D. B. Beach, and P. A. Holbert, J. Chem. Phys. **92**, 3144 (1990).
[9] S. M. Gates, C. M. Greenlief, and D. B. Beach, J. Chem. Phys. **93**, 7493 (1990).
[10] S. M. Gates and C. M. Greenlief, S. K. Kulkarni, and H. H. Sawin, J. Vac. Sci. Technol. A **8**, 2965 (1990).
[11] C. M. Greenlief, S. M. Gates, and P. A. Holbert, J. Vac. Sci. Technol. A **7**, 1845 (1989).
[12] S. M. Gates, Surf. Sci. **195**, 307 (1988).
[13] F. Bozso and Ph. Avouris, Phys. Rev. B **38**, 3943 (1988).
[14] R. Imbihl, J. E. Demuth, S. M. Gates, and B. A. Scott, Phys. Rev. B **39**, 5222 (1989).
[15] S. K. Kulkarni, S. M. Gates, B. A. Scott, and H. H. Sawin, Surf. Sci. **239**, 13 (1990).
[16] S. K. Kulkarni, S. M. Gates, C. M. Greenlief, and H. H. Sawin, Surf. Sci. **239**, 26 (1990).
[17] R. J. Hamers and Y. Wang, Chem. Rev. (Washington, D.C.) **96**, 1261 (1996).
[18] Y. Tsukidate and M. Suemitsu, Jpn. J. Appl. Phys., Part 1 **40**, 5206 (2001).
[19] J. H. G. Owen, K. Miki, D. R. Bowler, C. M. Goringe, I. Goldfarb, and G. A. D. Briggs, Surf. Sci. **394**, 79 (1997).
[20] X. L. Zhou and J. M. White, Appl. Surf. Sci. **35**, 52 (1988).
[21] K. M. Ogle, J. R. Creighton, S. Akhter, and J. M. White, Surf. Sci. **169**, 246 (1986).
[22] J. K. Kang and C. B. Musgrave, Phys. Rev. B **64**, 245330 (2001).
[23] R. D. Smardon and G. P. Srivastava, J. Chem. Phys. **123**, 174703 (2005).
[24] M. C. Payne and J. Joannopoulous, Rev. Mod. Phys. **64**, 1045 (1992).
[25] J. P. Perdew, K. Burke, and M. Ernzerhof, Phys. Rev. Lett. **77**, 3865 (1996).
[26] D. M. Bylander and L. Kleinman, Phys. Rev. B **41**, 907 (1990).